RSC Advances

PAPER

View Article Online
View Journal | View Issue

Cite this: *RSC Adv.*, 2022, **12**, 21122

Zinc binding strength of proteins dominants zinc uptake in Caco-2 cells†

Tian Li, Ruonan Jiao, Jiaqi Ma, Jiachen Zang, Guanghua Zhao and Tuo Zhang *

Zinc plays a vital role in structural, catalysis, and signal regulation in the human body. Zinc deficiency leads to the dysfunction of many organs and immunity systems. Diet proteins have distinct effects on zinc uptake. However, the mechanisms are uncovered. Here we select three principal components from whey protein: alpha-lactalbumin, beta-lactoglobulin, and bovine serum albumin, which bind with zinc at different affinities, to evaluate the relationship between their potential zinc uptake and protein binding. The experimental data shows that beta-lactoglobulin could promote zinc uptake, alpha-lactalbumin has minor effects, whereas bovine serum albumin reduced zinc uptake in Caco-2 cell lines. Zinc binding effects on protein structure were thoroughly inspected through fluorescent spectroscopy and X-ray crystallography. Isothermal titration calorimetry revealed that three proteins have different binding affinities toward zinc ions. We speculate that protein binding eliminates toxic effects from free zinc, and the binding strength dominates zinc uptake.

Received 9th June 2022
Accepted 17th July 2022

DOI: 10.1039/d2ra03565k

rsc.li/rsc-advances

1 Introduction

In adults, zinc content is 1.4–2.3 grams on average. It is the second most abundant trace element after iron.[1] Zinc is widely distributed in human tissues, with bone and skeletal muscle constituting the most significant proportion (~86%), followed by skin (~4.2%) and liver (~3.4%).[2] According to the Dietary Nutrient Reference Intake of Chinese Residents, normal adults were suggested to take in 15 mg of zinc daily, infants under 13 years old should take in 3–13 mg zinc daily, pregnant, and lactating women should take 20–25 mg zinc daily. Zinc content is high in cereals, eggs, and meat products, and the highest in oysters.[3,4] In the body, zinc binds mainly to proteins,[5] and the human genome predicts that about 3000 proteins bind to zinc ions.[2] Zinc ions primarily play roles in stabilizing protein structure and catalyzing metalloproteinase activity in human cells, and also in signal transduction as a second messenger.[6] Cell zinc levels need to be maintained steady state since zinc deficiency or excess can affect human health.

It is believed that zinc homeostasis is maintained in mammals mainly by two zinc transporters, ZnT and ZIP. The ZnT family (ZnT1–10) mediates zinc excretion from the cytoplasm, while the ZIP family (ZIP1–14) promotes zinc transport into the cytoplasm from the extracellular environment and intracellular vesicles.[7] These proteins have different distributions in various tissues and organs in the human body. The uptake of zinc in food is mainly realized by hZIP4, which located in the small intestinal villus epithelial cells, and ZnT1 releases the cytoplasm zinc ions into the human blood for utilization in the body.[8] Globally, almost 17% of the population is deficient in zinc, which leads to 4% of child mortality and morbidity.[9] Zinc is also closely associated with cardiovascular disease, cancer, Alzheimer's disease, depression *etc.*[10]. Zinc deficiency may cause issues with smell and taste disorders, immune system disorders, developmental delays, and affect the immune system.[10] In addition, excessive zinc ions can cause nausea, vomiting, loss of appetite, stomach-ache, and other symptoms.[11]

The body does not produce zinc independently and does not have dedicated zinc reserves, so it is necessary to uptake zinc from diet to maintain a steady state. Hence, zinc insufficient uptake and metabolic disorders can cause zinc deficiency. With the recognition of the importance of zinc, zinc supplements are constantly developing and updating, mainly going through four stages, from inorganic zinc, simple organic acid zinc, yeast zinc to protein zinc.[12] Compared with the previous three generations, protein zinc has the advantages of better stability, minor irritation, and high bioavailability in the human gastrointestinal tract.[12] Additionally, the protein zinc elements while increasing the intake of amino acids. So, protein zinc is now considered as the safest and most efficient zinc supplement.

Researchers found that protein consumption, particularly whey protein, improved zinc uptake in humans.[13] Whey protein is derived from bovine milk, which contains approximately 3% protein. Whey proteins are of two types: insoluble casein takes

College of Food Science and Nutritional Engineering, Key Laboratory of Precision Nutrition and Food Quality, Ministry of Education, China Agricultural University, Beijing 100083, China. E-mail: tuozhang@cau.edu.cn

† Electronic supplementary information (ESI) available. See https://doi.org/10.1039/d2ra03565k

up 80%, and others are soluble whey protein.[14] Zinc binds primarily to casein in infant formulas, while whey and fat only bind in small amounts. However, zinc bound to casein may lead to zinc clots that cannot be digested in the small intestine, leading to the low zinc uptake efficiency.[15] Whey protein is a whole-valent protein containing all the amino acids. Whey protein has high nutritional value and functional properties, such as regulating blood pressure, lowering cholesterol, antiviral, anti-cancer, antibacterial activity, and relieving mental stress.[16] The main components of whey proteins are beta-lactoglobulin (~46.6%), alpha-lactalbumin (~17.5%), lactoferrin (~11.7%), bovine serum albumin (~5.8%) and immunoglobulins (~2.9%).[17]

Beta-lactoglobulin (β-LG) is widespread in ruminant milk, which is generally composed of 162 amino acid residues and is 18 kDa in molecular weight.[18] It has good biological activity, such as antioxidant, anti-cancer, anti-aging, and immunity enhancement functions, and its enzymatic hydrolysates also have the function of lowering cholesterol levels. β-LG has various beneficial nutritional and functional food characteristics, and β-LG containing whey protein products, ingredients of choice in everyday foods and beverages.[19] Alpha-lactalbumin (α-LA) is widely distributed in the milk of mammals (cow, goat, camel, *etc.*) and humans. 123 amino acids are found in a single chain, and its molecular mass is ~14 kDa. α-LA functions in such as lactose synthesis, immunomodulation, *et al.*[18] α-LA is widely used in food industries, including infant formulas, protein-fortified beverages, lactose-free and reduced-carbohydrate foods, and medical foods.[19] There are 582 amino acid residues in bovine serum albumin (BSA) (~66 kDa), which comprises three similar domains (I, II, and III).

Studies have demonstrated that whey protein will bind with zinc ions through acidic amino acid residues as well as histidine through intrinsic fluorescence quenching and isothermal titration calorimetry (ITC).[20] Several zinc coordination structures have also been solved in α-LA, β-LG, and BSA.[21–23] Zinc binding to α-LA and β-LG was found to reduce zinc toxicity and promote zinc uptake. However, BSA binding reduced zinc to Caco-2 cells cytotoxicity meanwhile reduced zinc uptake. The mechanism under their similar zinc-binding but different zinc uptake efficiency was still unclear. In this research, we proved the phenomena of whey protein binding reducing the cell toxicity from zinc ions. Furthermore, we speculated on the detailed mechanism between protein zinc interaction and the zinc uptake efficiency. Finally, we proposed the zinc-binding strength dominating zinc uptake efficiency in Caco-2 cells. This study provides a reliable theoretical basis for using protein binding zinc as zinc nutritional supplements.

2 Material and methods

2.1 Materials

α-LA from bovine milk (PAGE electrophoresis pure purity ≧ 85%, molecular weight 14.17 kDa), β-LG from bovine milk (PAGE electrophoresis pure purity ≧ 90%, molecular weight 18.56 kDa) and bovine serum albumin (BSA, PAGE electrophoresis pure purity ≧ 97%, molecular weight 66.43 kDa) were purchased from Solarbio Life Science (Beijing, China).

Protein was used without further purification, and its powder was dissolved in pH 7.3 HEPES buffer (50 mM HEPES, 100 mM NaCl) at 25 °C. They were stored at 4 °C until used. $ZnSO_4 \cdot 7H_2O$ powder was dissolved in ultrapure water to obtain $ZnSO_4$ solution. They were stored at 25 °C until used.

2.2 Cell experiment

2.2.1 Cell culture and treatments. Caco-2 cell cultures were obtained from American Type Culture Collection (Rockville, Md., USA); Caco-2 cells were grown in Dulbecco's modified Eagle's medium, which contains streptomycin and penicillin (DMEM, purchased from Solarbio Life Science) supplemented with 15% fetal bovine serum (FBS, GIBCO). Each 25 cm^2 flask was incubated at 37 °C with humidified atmosphere 5% CO_2, until the cells grew to their desired density.

2.2.2 Cell proliferation and cytotoxicity assay. In addition to MTT, the Cell Counting Kit-8 (CCK-8) kit is an alternative method based on WST (water-soluble tetrazolium salt) widely used in proliferation cytotoxicity testing. WST was reduced to yellow formazan product by dehydrogenase in cells under the action of electron carrier, and the amount of formazan product was related to the number of living cells.

100 μL cell suspension was seeded at a 1×10^5 cells per mL density in 96-well plates for 24 h. Then, replace the culture medium with serum-free DMDM and add 10 μL sample (the final concentration of $ZnSO_4$ is 60 μM and the final concentration of α-LA, β-LG, BSA, and FBS is 1%). Each group was set up with six replicates. After incubating in the incubator for 6 h, add 10 μL CCK-8 solution to each well. The absorbance at 450 nm was measured after 1 hour incubation in the incubator using a microplate reader.

2.2.3 Establish Caco-2 cell monolayer model and determination of intracellular zinc uptake. 0.5 mL Caco-2 cells were seeded into the upper chamber in 12-well transwell dishes (Corning Costar Co., Cambridge, MA) at a density of 2×10^5 cells per mL in serum-containing DMEM and 1.5 mL serum-containing DMEM was added to the lower chamber. Each medium was changed the other day, and every day after seven days. The monolayers' transepithelial electric resistance (TEER) was determined using the Millicell ERS-2 system (Millipore Corp., New Bedford, MA, USA). Experiments on zinc uptake were conducted when the cells had TEER values over 1000 Ω cm^2.

The assay was performed after Caco-2 cells were incubated for one hour with DMEM containing 2% FBS. The cells were then washed three times with Dulbecco's–Hanks balanced salt solution (D–Hank's). Then, add 0.5 mL samples (the final concentration of $ZnSO_4$ is 40 μM, and the final concentration of α-La, β-LG, and BSA is 1%) to the upper chamber and 1 mL D–Hank's to the lower chamber. Each group was set up with three replicates. After 2 h incubation in the incubator, the lower chamber samples were collected and cleaned once with 0.5 mL D–Hank's and combined. The zinc content was detected by

inductively coupled plasma mass spectrometry (ICP-MS, Agilent 7800 ICP-MS, USA).

2.3 Fluorescence spectrometry

Fluorescence spectroscopy is an important tool when analyzing protein–zinc interactions. In this case, α-LA concentration was 20 μM, stock $ZnSO_4$ concentration was 43.2 mM, and the molar ratio of Zn/α-LA was 0, 24, 48, 72, 96, 120 during titration. β-LG concentration was 20 μM, stock $ZnSO_4$ concentration was 28.8 mM and the molar ratio of Zn/β-LG was 0, 16, 32, 48, 64, 80, 96, 112, 128, 160 during titration. BSA concentration was 5 μM, stock $ZnSO_4$ concentration was 24 mM and the molar ratio of Zn/BSA was 0, 53, 107, 160, 213, 267, 320, 373 during titration. Each titration, 10 μL $ZnSO_4$ solution was titrated to a 900 μL protein solution in a 1.0 cm quartz cuvette, and totally 50 μL, 90 μL and 70 μL $ZnSO_4$ were titrated α-LA $ZnSO_4$, β-LG and BSA, respectively. The fluorescence spectra of the solution were scanned on an F-4500 fluorescence spectrophotometer (Hitachi Ltd., Tokyo, Japan) at 298 K. The excitation wavelength was 280 nm, and the emission wavelength was measured from 290 to 450 nm at a slow scan rate. Both the widths of the excitation and emission slits were set at 5 nm. All the experiments were carried out in triplicate. Analysis of the collected data was performed using Origin 2021 software (OriginLab, Northampton, MA, USA).

2.4 Protein crystallization, data collection, and structure determination

First, wizard 1 & 2 and wizard 3 & 4 crystallizing screening kits were used to screen the initial crystallizing conditions. Then, the crystallization conditions were optimized. In the optimization experiment, the sitting drop vapor diffusion method was used to culture the crystals, and the pH of the culture conditions and the concentration of precipitant were mainly adjusted. All crystal screening and optimization were performed in a 20 °C constant temperature incubator. α-LA was crystallized in the solution with 30% MPD, 100 mM imidazole pH 6.5, 200 mM $(NH_4)_2SO_4$ and 10% PEG 3350. β-LG was crystallized in the solution with 20% PEG 3350, 50 mM HEPES pH 7.3, 200 mM NH_4HCO_2.

The crystals were picked up by using nylon rings and placed in the cryoprotect medium with 25% glycerol for a few seconds, then directly frozen in liquid nitrogen. Glycerol acts as an antifreeze to prevent the formation of ice crystals. Crystal diffraction images were collected at Shanghai Synchrotron Radiation Facility (SSRF). The diffraction data were indexed and scaled by using HKL3000 software.

Molecular replacement was used to determine the structures in Phenix by using the Phaser-MR program. With phenix.refine, the structure was refined, and then rebuilt with COOT, with manual adjustments. All the resulting figures in this manuscript were created with PyMOL.

2.5 Isothermal titration calorimetry (ITC)

ITC can directly measure the heat change during the binding process of two substances at constant temperature and analyze the driving binding process and intermolecular interactions.[24] Thermodynamic parameters of zinc-binding with α-LA, β-LG and BSA at 25 °C were determined using Nano ITC (TA Instruments, New Castle, Delaware, USA). When protein and zinc bind, they will either absorb or exotherm heat according to the type of reaction. Furthermore, thermodynamic parameters can be obtained by ITC measurement of heat. 200 μL of protein solution (157.8 μM α-LA; 92.9 μM β-LG; 87 μM BSA) was loaded into the sample cell and 50 μL of $ZnSO_4$ solution (6 mM) into injection syringes. Before titration, all solutions were vacuum degassed for 20 minutes. This experiment involved 17 successive injections of $ZnSO_4$ solution into the reaction cell, and each injection was 2 μL, without counting the first injection. The constant mixing speed (300 rpm) and a 200 second time delay were set to ensure proper mixing after each injection. The dilution heat during the titration $ZnSO_4$ (6 mM) into buffer (50 mM HEPES, 100 mM NaCl pH 7.3) was also measured and subtracted from the raw data. Data collection and analysis were performed by NanoAnalyze (TA Instruments, New Castle, Delaware, USA) and further fitted to the model "independent-binding-site" or "multiple-binding-sites" model. To find the thermodynamic parameters, the binding isotherms were iteratively fitted to determine the affinity constants (K_d), binding stoichiometry (N), enthalpies (ΔH), and entropies (ΔS) changes. The Gibbs free energy difference was calculated by using the equation ($\Delta G = \Delta H - T\Delta S$).

2.6 Statistical analysis

For each of the treatment groups, mean values and standard deviations were calculated. *R* 4.0.5 was used for data analysis, package "outliers" was used to analyse and eliminate outliers (Grubb's method), package "agricolae" was used for significant difference analysis, and error limits were calculated.

3 Results and discussion

3.1 The effect of whey protein components binding on zinc uptake in Caco-2 cells

It has been well established that zinc is the essential micronutrient, whereas excess zinc has toxic side effects on the cell and human body.[10,11] All protein-binding zinc was proved to protect the cell from free zinc toxicity. However, different proteins show variant zinc uptake efficiency. Whey protein as a protein complex has positive effects on zinc uptake and utilization. Meanwhile, the components such as α-LA, β-LG, and BSA are considered to play different roles, sometimes contrary roles on zinc uptake when they bind zinc as the zinc supplements under different conditions.[25,26]

To system evaluate the effects of whey protein components on zinc uptake and investigate the mechanism of the different effects from different consonants, α-LA, β-LG, and BSA were selected as zinc-binding supplements and their zinc uptake efficiency was investigated through the well-established monolayer Caco-2 cell uptake model. The toxicity of the three protein–zinc complexes was determined using the CCK-8 kit. As shown in Fig. 1A, 60 μM free zinc was toxic to cells, and less than 80%

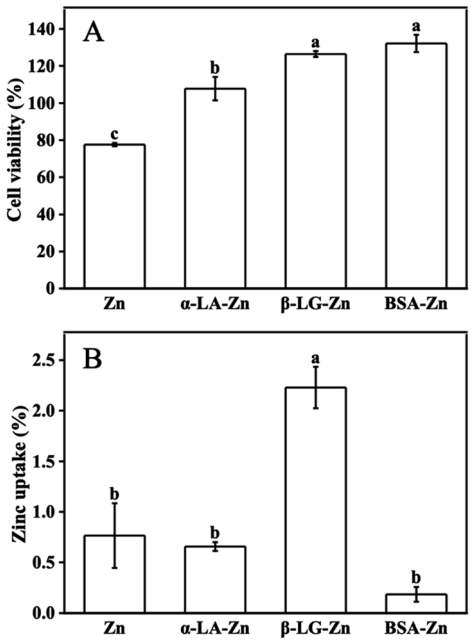

Fig. 1 Zinc toxicity and uptake efficiency. (A) The effects of α-La, β-LG, BSA, and FBS binding zinc on cell viability which were detected by CCK-8. Caco-2 cells were treated with 60 μM $ZnSO_4$ and 1% α-LA, β-LG, BSA for 6 h, and the free zinc ions group was set as control. (B) Zinc uptake by α-LA, β-LG, and BSA binding in Caco-2 monolayer cells. Caco-2 cells were treated with 40 μM $ZnSO_4$ and 1% α-LA, β-LG, BSA for 2 h, and the free zinc ions group was set as control.

cell viability was observed. When the same amount of zinc was supplied with 1% α-LA, β-LG, and BSA binding, the toxicity from free zinc was eliminated. This result proved the protein binding reduced the free zinc concentration in the medium and further reduced the toxic effects of excess free zinc ions, consistent with the previous reports.[26] Therefore, the complexes of these three protein and zinc were safe to be used in the following uptake experiments.

To study the uptake of zinc across the intestinal barrier, Caco-2 differentiated monolayer model was used. The same amount of zinc ions was added to the upper chamber of the transwell plates. Interestingly, significant different zinc concentrations were observed in the lower chamber (Fig. 1B). Zinc transported from the α-LA–zinc was similar to the free zinc group. The addition of BSA reduced the uptake of zinc. However no statistically significant difference was observed. In the β-LG–zinc treatment group, the zinc uptake was significantly increased compared with three other treatments. Since the protein used in this experiment was excess toward zinc ions, and all three proteins are rich in metal coordination amino acids, the different zinc uptake efficiency should come from different binding strength and different coordination between protein and zinc ions.

3.2 Intrinsic fluorescence effects of whey protein components with zinc binding

Proteins produce intrinsic fluorescence at specific excitation wavelengths from their aromatic amino acids. Of the three aromatic amino acids, tryptophan (Trp) and tyrosine (Tyr), especially Trp play the dominant role in intrinsic fluorescence, whereas phenylalanine (Phe) was always ignored due to its low quantum yield.[27] Fluorescence titration was an efficient and reliable method to test protein interaction with metal ions, since metal-binding will induce protein local tertiary structure change, which could be observed by monitoring the protein intrinsic fluorescence intensities. Among the three components, α-LA contains four Trp and four Tyr residues, β-LG has two Trp and four Tyr residues, and BSA owns two Trp and twenty Tyr residues in each subunit.

As free zinc ions were continually titrated into protein solution, the three proteins showed different intrinsic fluorescence responses, which reflect their different tertiary structure response in binding with zinc ions (Fig. 2). With the titration of zinc sulphate, the intrinsic fluorescence intensity of α-LA significantly increased as well as a redshift from 325 nm to 335 nm (Fig. 2A). The maximum emissions wavelength of the of Trp residues depends on the polarity of their microenvironment.[28] The redshift fluorescence indicated that the polarity around the Trp residues increased. Namely, the Trp residues are exposed to an environment that is more hydrophilic. However, after the continuous addition of zinc sulphate, the fluorescence

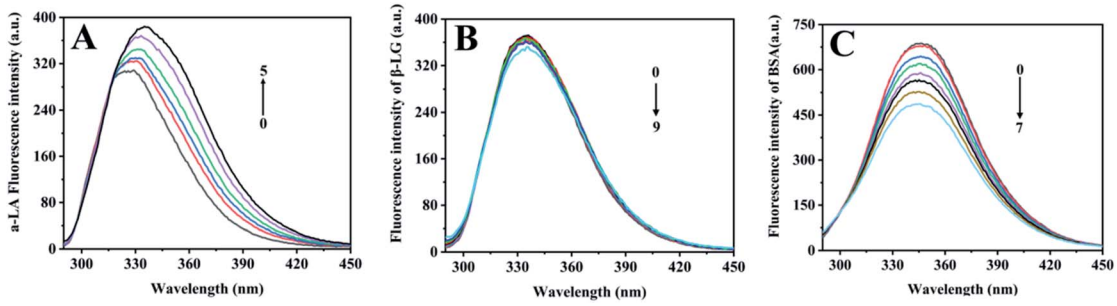

Fig. 2 Fluorescence titration of zinc ions into whey protein components. (A) Fluorescence changes of α-LA during the addition of zinc. 10 μL $ZnSO_4$ (43.2 mM) solution was titrated to 900 μL α-LA (20 μM) each titration. (B) Fluorescence changes of β-LG during the addition of zinc. 10 μL $ZnSO_4$ (28.8 mM) solution was titrated to 900 μL β-LG (20 μM) each titration. (C) Fluorescence changes of BSA during the addition of zinc. 10 μL $ZnSO_4$ (24 mM) solution was titrated to 900 μL BSA (5 μM) each titration. The numbers in the figure represent the titration times of each experiment.

intensity of β-LG did not change significantly (Fig. 2B). This result suggested that Zn^{2+} had slightly influenced the tertiary structure of β-LG. With the drop of zinc sulphate solution, the intrinsic fluorescence intensity of BSA was significantly quenched (Fig. 2C), which indicated a relatively strong interaction between zinc and coordination residues.

3.3 Detailed coordination structure of zinc binds with whey protein components

To illustrate the detailed zinc coordination environments of the three whey protein components, the zinc-binding protein complex crystals were cultured, and the crystal structures were solved through X-ray crystallography. Crystallization conditions were screened and optimized to obtain crystals that are suitable for X-ray diffraction to obtain structural information at the atomic level. α-LA and β-LG with zinc-binding crystal structures were successfully solved at the resolution of 2.5 Å and 2.0 Å, respectively. The crystallographic statistics generated from this work were shown in ESI Table 1,† and zinc bonded protein structures were deposited into WWPDB bank, with PDB ID 7WQG and 7WQL for α-LA and β-LG, respectively.

In a single α-LA subunit, there are two zinc binding sites were identified in the crystal structure (Fig. 3A). There are five amino acid residues (Lys 79, Asp 82, Asp 84, Asp 87, Asp 88) were involved in zinc binding site (a), and the zinc coordination number is six. This binding site has been reported in a human α-LA crystal structure.[22] α-LA was reported to be the only whey protein that binds with Ca^{2+}, and this binding site was previously reported to binding with a calcium ion. However, the Ca^{2+} can be replaced with Zn^{2+} when soaking with zinc ions.[22] The other zinc loosely coordinated with Asn44, which could be a nonspecific weak binding site (b) since it was only found in one subunit out of the five subunits in one symmetry unit.

Five zinc-binding sites are identified in the β-LG crystal structure, and the binding sites are in the four vertices of the regular tetrahedral-like β-LG structure (Fig. 3B). The detailed coordination of these five zinc ions is shown in Fig. 3B. There are a bunch of His and acidic amino acids all around the β-LG surface, which could bind with zinc ions, and our result proved the existence of these zinc-binding sites. Sauter and co-workers investigated the crystallization pathways in the presence of the di- and trivalent salts ($ZnCl_2$ and YCl_3) by using bovine β-LG as a model.[23] Constant with the published crystal structure, two zinc-binding sites (a and c) were also identified in this research.[23] Furthermore, three more zinc-binding sites (b, d and e) were identified in this research, which has not been reported in previous research.

Unfortunately, the BSA–zinc binding structure was solved at 4.5 Å, and the detailed zinc coordination was not confidently identified. A published equine serum albumin (ESA)–zinc-binding structure were used to analysis zinc coordinations.[21] There are ten zinc binding sites have been identified in equine serum albumin (ESA).[21] Serum albumin was considered to be metal vehicles in the blood.[29] Serum albumin from human and equine structures were also determined with zinc ion binding.[21] Two strong binding sites from ESA are shown in Fig. 3C. Considering the sequence between BSA and ESA has an 86.16% similarity and 74.46% identity (**https://uniport.org**), the BSA should conserve similar zinc-binding properties.

Cysteine, histidine, aspartate, and glutamate residues are the most common zinc-binding residues. According to Tang *et al.*, the zinc-binding site composed of multiple aspartates and glutamates was too flexible and exhibited weak binding constants due to fast zinc dissociation.[20] In order for zinc to bind strongly to proteins, aspartate and glutamate must combine with other nitrogen donors (histidine) or sulphur donors (cysteine).[20] These observations indicate that zinc binds to these residues have been observed in the co-crystallized structures in this study. For uptake of zinc in the intestines, the coordination environments of zinc ions dominate the binding affinity between zinc ions and proteins, which may have different effects on zinc release from binding proteins to zinc transporters, and further have different uptake efficiency during Caco-2 cell monolayer transport.

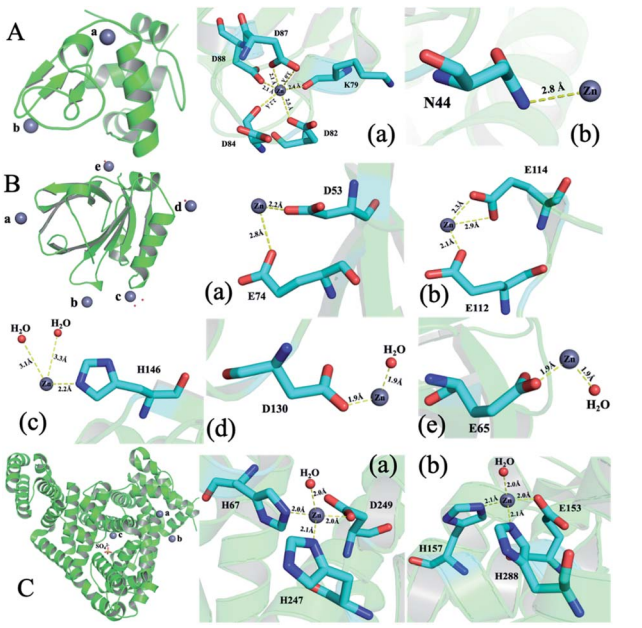

Fig. 3 The structure of whey protein components and binding sites coordination around zinc ions. (A) α-LA (PDB ID: 7WQG). (B) β-LG (PDB ID: 7WQL). (C) ESA (PDB ID: 5IIU).

3.4 The thermodynamic study of zinc binding with whey protein components

The thermodynamic and binding strength between zinc and three whey protein components was evaluated with isothermal titration calorimetry. In the ITC experiment, heat flow was measured when zinc ions were injected into the protein solution. Fig. 4 plots the heat changes *versus* the injection times of zinc into α-LA, β-LG, and BSA at 25 °C, and the peak areas were integrated.

The thermodynamic parameters (K_d, N, ΔH, and ΔS) were calculated according to the software NanoAnalysis and the corresponding results were shown in Table 1. According to

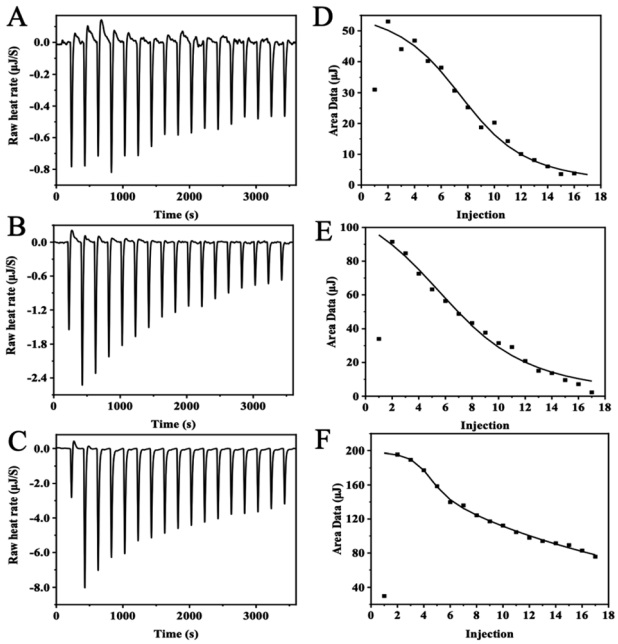

Fig. 4 ITC data of zinc-binding to whey proteins. Titration curves of titrating 6 mM $ZnSO_4$ to 157.8 μM α-LA (A), 92.9 μM β-LG (B) and 87 μM BSA (C); integration of the thermogram yielded zinc-binding isotherm graphs of α-LA (D), β-LG (E) and BSA (F).

Table 1, the negative values of ΔG indicate that the interaction of zinc with α-LA, β-LG, and BSA was spontaneous. ΔH and ΔS were higher than 0, indicating that the significant heat source during interaction comes from hydrophobic forces. Besides, the binding of zinc to these three proteins is entropy-driven ($\Delta H > 0$, $\Delta S > 0$, $\Delta G < 0$) endothermic reaction ($\Delta H > 0$).[20]

α-LA and β-LG titration data were fitted into an "independent-binding-site" model, and the BSA binding zinc titration was fitted with the "multiple-binding-sites" model. According to the ITC data, α-LA binding with three zinc ions, and β-LG coordination with five zinc ions, which are consistent with the crystal structure data. The affinity of zinc toward α-LA is relatively strong at $K_d = 5.68 \times 10^{-5}$ M. Meanwhile, β-LG binding with zinc ions much weaker at the $K_d = 1.22 \times 10^{-4}$ M. BSA has two binding sites with different affinities, a strong binding site ($N = 3$, $K_d = 7.00 \times 10^{-6}$ M) and a weak binding site ($N = 7$, $K_d = 2.00 \times 10^{-3}$ M). In general, the values agree with previous studies.[27] Since protein concentration was excess over zinc ions, the N number will not affect the zinc uptake experiment, whereas the binding affinity dominates the zinc uptake efficiency in Caco-2 cells.

Table 1 Thermodynamic parameters of zinc-binding to α-LA, β-LG and BSA at 25 °C measured by ITC

	N	K_d (10^{-5} M)	ΔH (kJ mol^{-1})	ΔS (J mol^{-1} K^{-1})	ΔG (kJ mol^{-1})
α-LA	3	5.68	4.83	97.46	−24.23
β-LG	5	12.20	10.32	109.50	−22.33
BSA	3	0.70	16.47	153.90	−29.42
	7	200.00	50.41	221.00	−15.49

Diet protein will bind with zinc ions through specific amino acid residues, which will significantly reduce the free zinc concentration in the solution. Hence the free zinc toxicity was eliminated. Protein-bonded zinc will release to transporters in the small intestine to facilitate zinc uptake, whereas proteins, like BSA with strong-binding sites, will impede zinc sufficiently release due to competitive binding over transporters. The binding strength is sensitive to many environmental conditions, such as temperature, buffer solutions, pH values, *et al.* It is not rigorous to draw a confidant K_d number over zinc uptake in Caco-2 cell models. However, it is evident that, under similar conditions, diet proteins that bind zinc weakly will promote zinc uptake, and proteins that have stronger binding than β-LG will likely inhibit zinc uptake.

4 Conclusions

Zinc was found to interact with whey protein components α-LA, β-LG, and BSA in this study in a comprehensive and specific way. Fluorescence spectroscopy analysis revealed that zinc leads to a redshift in the spectra maxima of α-LA, and the tertiary structure of α-LA has changed. Zinc quenches the intrinsic fluorescence of BSA, while β-LG has little effect. The crystal structure results further characterized the specific zinc-binding sites in these whey protein components. Furthermore, the ITC data analysis suggested that the bonding number between zinc with whey protein components was well aligned with crystal structures. In the present study, the binding number, strength, and mechanism of α-LA, β-LG, and BSA to zinc were explained detailly. For the first time to illustrate that although diet proteins could reduce the free zinc toxicity, they have variant effects on zinc uptake over Caco-2 cell monolayers. These studies are helpful to the research of zinc uptake and will promote the development of zinc supplements.

Author contributions

Tian Li: methodology, formal analysis, writing-original draft. Ruonan Jiao, Jiaqi Ma: methodology, formal analysis. Jiachen Zang, Guanghua Zhao: supervision, writing review & editing. Tuo Zhang: conceptualization, data analysis, supervision, writing review & editing, project administration.

Conflicts of interest

The authors declare that they have no known competing financial interests or personal relationships that could have appeared to influence the work reported in this paper.

Acknowledgements

This work was supported by the National Natural Science Foundation of China (No. 31901638) and the 2115 Talent Development Program of China Agricultural University (No. 109027). The Shanghai Synchrotron Radiation Facility (SSRF) is especially acknowledged for beam time. We thank the staffs from BL17U1/BL18U1/19U1 beamline of the National Center for

Protein Sciences Shanghai (NCPSS) at Shanghai Synchrotron Radiation Facility for assistance during data collection.

References

1 C. T. Chasapis, P.-S. A. Ntoupa, C. A. Spiliopoulou and M. E. Stefanidou, *Arch. Toxicol.*, 2020, **94**, 1443–1460.
2 M. Maares and H. Haase, *Nutrients*, 2020, **12**, 762.
3 J. Li, C. Gong, Z. Wang, R. Gao, J. Ren, X. Zhou, H. Wang, H. Xu, F. Xiao, Y. Cao and Y. Zhao, *Mar. Drugs*, 2019, **17**, 341.
4 H. Scherz and E. Kirchhoff, *J. Food Compos. Anal.*, 2006, **19**, 420–433.
5 A. Rodzik, P. Pomastowski, G. N. Sagandykova and B. Buszewski, *Int. J. Mol. Sci.*, 2020, **21**, 2156.
6 Y. Tamura, *J. Atheroscler. Thromb.*, 2021, **28**, 1109–1122.
7 T. Kambe, T. Tsuji, A. Hashimoto and N. Itsumura, *Physiol. Rev.*, 2015, **95**, 749–784.
8 T. Kimura and T. Kambe, *Int. J. Mol. Sci.*, 2016, **17**, 336.
9 M. E. Penny, *Ann. Nutr. Metab.*, 2013, **62**, 31–42.
10 C. T. Chasapis, A. C. Loutsidou, C. A. Spiliopoulou and M. E. Stefanidou, *Arch. Toxicol.*, 2012, **86**, 521–534.
11 K. E. Levine, B. J. Collins, M. D. Stout, M. Wyde, S. E. Afton, A. S. Essader, T. J. Ennis, K. E. Amato, A. C. McWilliams, B. L. Fletcher, R. A. Fernando, J. M. Harrington, N. Catlin, V. G. Robinson and S. Waidyanatha, *Anal. Lett.*, 2017, **50**, 2447–2464.
12 M. C. Udechukwu, S. A. Collins and C. C. Udenigwe, *Food Funct.*, 2016, **7**, 4137–4144.
13 H. O. Santos, F. J. Teixeira and B. J. Schoenfeld, *Clin. Nutr.*, 2020, **39**, 1345–1353.
14 A. Haug, A. T. Høstmark and O. M. Harstad, *Lipids Health Dis.*, 2007, **6**, 25.
15 M. L. Pabón and B. Lönnerdal, *J. Trace Elem. Med. Biol.*, 2000, **14**, 146–153.
16 B. B. Solak and N. Akin, *J. Food Eng.*, 2012, **3**, 1–7.
17 L. Giblin, A. S. Yalçın, G. Biçim, A. C. Krämer, Z. Chen, M. J. Callanan, E. Arranz and M. J. Davies, *Free Radical Res.*, 2019, **53**, 1136–1152.
18 C. Zhao, N. Chen and T. J. Ashaolu, *Int. Dairy J.*, 2022, **126**, 105269.
19 T. Lin, G. Meletharayil, R. Kapoor and A. Abbaspourrad, *Nutr. Rev.*, 2021, **79**, 48–69.
20 N. Tang and L. H. Skibsted, *Food Res. Int.*, 2016, **89**, 749–755.
21 K. B. Handing, I. G. Shabalin, O. Kassaar, S. Khazaipoul, C. A. Blindauer, A. J. Stewart, M. Chruszcz and W. Minor, *Chem. Sci.*, 2016, **7**, 6635–6648.
22 J. Ren, D. I. Stuart and K. R. Acharya, *J. Biol. Chem.*, 1993, **268**, 19292–19298.
23 A. Sauter, M. Oelker, G. Zocher, F. Zhang, T. Stehle and F. Schreiber, *Cryst. Growth Des.*, 2014, **14**, 6357–6366.
24 X. Du, Y. Li, Y.-L. Xia, S.-M. Ai, J. Liang, P. Sang, X.-L. Ji and S.-Q. Liu, *Int. J. Mol. Sci.*, 2016, **17**, 144.
25 S. R. Drago and M. E. Valencia, *J. Agric. Food Chem.*, 2004, **52**, 3202–3207.
26 M. Maares, A. Duman, C. Keil, T. Schwerdtle and H. Haase, *Metallomics*, 2018, **10**, 979–991.
27 S. Bi, B. Pang, T. Wang, T. Zhao and W. Yu, *Spectrochim. Acta, Part A*, 2014, **120**, 456–461.
28 J. R. Albani, *Spectrochim. Acta, Part A*, 1998, **54**, 175–183.
29 J. Hu, E. Hernandez Soraiz, C. N. Johnson, B. Demeler and L. Brancaleon, *Int. J. Biol. Macromol.*, 2019, **134**, 445–457.